

Thermochromic ink–paper interactions and their role in biodegradation of UV curable prints

Marina Vukoje  · Snežana Miljanić · Jasna Hrenović · Mirela Rožić 

Received: 8 November 2017 / Accepted: 1 August 2018 / Published online: 10 August 2018
© Springer Nature B.V. 2018

Abstract In this study, biodegradability aspects of UV thermochromic leuco dye print on three different paper materials (synthetic, recycled, and bulky) were studied using the soil burial test under anaerobic conditions. Biodegradation of UV curable thermochromic prints were evaluated for changes by visual examination, microbial growth assay, weight loss measurements, Fourier transform infrared spectroscopy, scanning electron microscopy and colorimetric measurements. Results showed a better absorption of ink into the bulky paper structure, followed by recycled paper. Synthetic paper is not absorbent. The ink binder altogether with classic pigment and microcapsules penetrates into the structure of bulky paper. Recycled paper absorbs ink binder mostly with classic pigment. Better adsorption of binder into the bulky paper structure results in thinner layer of ink binder on the paper surface. On non-absorbent synthetic paper, microcapsules are covered

with thicker layer of ink binder. In the case of bulky paper, the highest rate of biodegradation was observed, resulting in a higher number of bacteria, higher weight loss, higher changes in colour (destruction of almost all microcapsules) and almost complete reduction in thermochromic effect of the prints. Results show that microcapsules, which penetrate into the structure of bulky paper, are promoting the rate of bulky paper biodegradation. The opposite behaviour was noticed for the penetration of classic pigment into the structure of recycled paper, which resulted in remarkable reduction of recycled paper biodegradation rate. The thicker layer of ink binder (containing classic pigment) on the surface of microcapsules on recycled paper resulted in slower rate of microcapsules degradation and smaller colour change of the print. The thickest layer of ink binder and classic pigment on synthetic paper surface causes the slowest rate of biodegradation of print.

Keywords Thermochromic ink · Paper ink interactions · Biodegradation · Bacteria · SEM · FTIR

M. Vukoje · M. Rožić (✉)
Faculty of Graphic Arts, University of Zagreb,
Getaldićeva 2, 10 000 Zagreb, Croatia
e-mail: mirela.rozic@grf.hr

S. Miljanić
Department of Chemistry, Faculty of Science, University
of Zagreb, Horvatovac 102a, 10 000 Zagreb, Croatia

J. Hrenović
Department of Biology, Faculty of Science, University of
Zagreb, Rooseveltov trg 6, 10 000 Zagreb, Croatia

Introduction

Printing inks are coloured complex mixtures, liquids or pastes, mostly consisting of colorant (pigments or dyes), binder (resins), solvent (organic or water based)

and additives (chelating agents, anti-oxidants, surfactants, biocides, etc.). Their composition and physical properties differ mostly due to printing processes for which they are intended. When it is applied to substrate, the ink must be converted to solid state. The binder dries and binds the colorants to the substrate. The drying of printing inks must be achieved as quickly as possible and it can be performed by physical (evaporation) and chemical (oxidation, radiation-induced curing) means or a combination of both (Leach 2007). Radiation-induced drying includes ultraviolet radiation, infrared, electron beam, microwave and radio frequency. The volatile organic compounds (VOC) evaporation from solvent based inks and their emission into the atmosphere during printing can be avoided by the use of water based and UV-cured inks. Besides better environmental aspects, the UV curable printing inks are especially suited for printing on non-absorbent surfaces due to quick drying (Robert 2015). Radiation curing inks are formulated as other inks, consisting of pigments, binder, solvent and additives. In UV curable printing inks the binders are generally acrylates (epoxy, polyurethane and polyester acrylates). The solvents in these systems are low-viscosity monomers while the additives can be waxes, surfactants, photoinitiators (e.g. benzophenone) and photoactivators (e.g. amines), inhibitors and in some cases additives to improve printability. Photoinitiators are required in order to achieve solid state of ink after printing, in the presence of UV light by free radical, cationic or hybrid reaction (Leach 2007). The UV curable printing inks have some drawbacks such as contamination of packaging by reactive diluents and photoinitiators which remain in the ink after printing (Robert 2015), as well as problems during recycling of paper (Carré et al. 2005).

In the last decade, there is an increasing demand for inks in packaging resulting in the growing of the printing ink market by 3% per year which leads to an increasing demand for traditional as well as new printing inks (Robert 2015). Recently, smart polymers, such as thermochromic printing inks can be found for application in different products.

Thermochromic printing inks change their colour by the heat. Commercially available thermochromic printing inks instead of classic pigments contain microencapsulated leuco dye–developer–solvent systems (Tang and Stylios 2006; Seeboth and Lotzsch 2013). The microencapsulated thermochromic

pigments usually have medium particle size of a few micrometres, which is about ten times larger than the particle size of conventional pigment particles (Seeboth and Lotzsch 2013). The thermochromic effect is caused by the formation of leuco dye–developer complexes in a reversible equilibrium redox reaction between leuco dye and developer (Seeboth et al. 2007). The reaction is triggered by interactions between the complex and the solvent during the melting or crystallization process. Leuco dye–developer–solvent systems are coloured in the solid state and transform on heating above the solvent melting temperature (activation temperature T_A) into a colourless liquid (Homola 2008). The most widely used system for microencapsulation of thermochromic inks involves urea-formaldehyde, melamine-formaldehyde, gelatine–gum arabic and epoxy resins (Aitken et al. 1996; Fujinami 1996; Seeboth and Lotzsch 2008). Melamine-formaldehyde resins are biodegradable and during biodegradation can act as carbon and nitrogen sources (El-Sayed et al. 2006).

In order to reduce the generation of municipal solid waste on landfills, different material recycling potentials for paper-based products have been purposed during last decade. Material recycling by flotation deinking is the most studied method for graphic papers, purposed for production of recycled fibres. Sometimes, this method is not suitable. For example for products contaminated with food (Monte et al. 2009). Besides this problems, some problems related to health safety of recycled paper due to residual printing inks in recycled pulp are of major concerns (Pivnenko et al. 2015). In order to avoid these problems, potentials of organic recycling should also be examined for new materials that can be found on the market. UV inks are generally known to cause problems during paper recycling resulting in residual ink in recycled pulp. The use of thermochromic printing inks is growing and they are being used for different applications, due to their attractive visual effects.

Biodegradability aspect of paper and paper based products was the subject of many studies (Venelampi et al. 2003; López Alvarez et al. 2009; De la Cruz et al. 2014; Wang et al. 2015). However, there is lack of knowledge about the biodegradation of printing inks and their influence on paper based products biodegradation. In some studies the printing inks are only referred to only as the toxic components (López

Alvarez et al. 2009; Hermann et al. 2011). Stinson and Ham (1995) studied a decomposition of printed and unprinted newspaper and based on the generated amount of methane the obtained results indicate that the printing ink did not inhibit the amount or affect the rate of methane production from cellulose in newspaper.

Studies of vegetable based polymers and binders biodegradation, which are commonly used in printing inks, have been investigated by few researches (Erhan and Bagby 1995; Erhan et al. 1997; Shogren et al. 2004) and also there are few available data on biodegradation of printed polymer films in which the reduction of biodegradation rate was noticed for printed samples (Hoshino et al. 2003; Bardi et al. 2014).

Our previous research has shown that biodegradation of thermochromic offset prints which dries by oxypolymerization of vegetable oil depends mostly upon physico-chemical properties of used paper substrates and absorption of ink binder into the paper structure (Vukoje et al. 2017).

Since several studies (Erhan and Bagby 1995; Erhan et al. 1997; Shogren et al. 2004) showed that differences in biodegradation of printing inks binders depends even upon small changes in their chemical composition, our goal was to investigate the differences in biodegradation of UV curable prints since they have different composition compared to offset prints.

Materials and methods

Printing substrate and printing ink

Three different paper substrates (synthetic, 33% recycled, and bulky), unprinted and printed with screen thermochromic ink were exposed to anaerobic soil conditions. Synthetic paper (Yupo, 73 g/m²) extruded from polypropylene pellets, recycled paper (Mondi, 80 g/m²) containing 33% of recycled cellulose fibres and bulky paper (Munken Print White, 80 g/m²) containing wood free pulp and more than 10% mechanical wood pulp, were used. These papers were selected due to their different chemical composition and absorption capacity.

For the printing of paper samples one leuco dye based, UV curable screen printing thermochromic ink

was used (Chromatic Technologies, Inc.). The activation temperature of thermochromic ink is 31 °C. Below its activation temperature, the thermochromic UV curable screen print (hereinafter UV print) was coloured in purple and above its activation temperature the print was coloured in pink. The printing ink was screen printed using the screen printing device (Holzschuher K.G., Wuppertal) employing 60/64 mesh. All the samples were printed in the full tone. The printed samples were dried under the UV irradiance (30 W/cm) using Technigraf Aktiprint L 10-1 device.

Air permeance (porosity) of paper samples

The air permeance (porosity) measurements were conducted using Frank Bendtsen Roughness Tester device according to the ISO 5636/3 standard method (Thompson 2004). Average values of ten measurements are presented as mean ± SD.

Determination of paper and print thickness

Thickness of unprinted paper samples was determined according to ISO 534:2005 standard using Enrico Toniolo DGTB001 Thickness Gauge. Print thickness values were obtained by subtracting the measured values of the thickness of unprinted paper from the measured values of thickness of paper with print. Average values of twenty measurements are presented as mean ± SD.

Soil burial experiments

Laboratory soil burial experiments were conducted at room temperature 25 ± 2 °C by placing the unprinted and printed papers horizontally in the forest field soils (containing humus) in glass containers. They were buried for 50 and 180 days, two samples of each. The water content of the soil was adjusted to 40% of its maximum water retention capacity. The commercial available reagent *Anaerocult A* (Merck) was used in order to allow the development of anaerobic conditions.

Scanning electron microscopy

The printed thermochromic surface before and after 180 days of biodegradation was monitored using a FE-

SEM Jeol 7000 field emission scanning electron microscope. The micrographs were taken under a magnification of 1000× and 5000×.

Optical microscopy

Microscopic image of thermochromic ink was taken using Olympus BX51 System Microscope under a magnification of 2000×.

Visual evaluation

A method of visual evaluation can be used in order to describe biodegradation as a first indication of microbial activity in the terms of visible surface changes such as formation of holes or cracks, de-fragmentation or changes in colour but it does not prove the existence of biodegradation process in terms of metabolism (Shah et al. 2008). Paper samples were taken out from the containers in sampling times and photos of them were made in order to visually evaluate the prints degradation over time. All the images were taken using Huawei camera under the same lighting conditions (resolution 3968 × 2976, CMOS BSI sensor, f/2.2, with a camera stand).

Fourier transform infrared (FTIR) spectroscopy

Infrared spectra in transmission and attenuated total reflectance (ATR) mode were measured using a Bruker Equinox 55 interferometer. The transmission IR spectra of the UV thermochromic printing ink were obtained at 25 and 50 °C from the sample smeared in a thin layer on the surface of the KBr pellet. For the temperature dependent measurements a Bruker heating device Eurotherm 2216e was used. The IR spectra were recorded in the spectral range between 4000 and 400 cm⁻¹ at 4 cm⁻¹ resolution and averaged over 32 scans. The baseline was corrected in the final spectrum. The ATR spectra of the paper samples, unprinted as well as printed with the ink before and after the soil burial, were measured using the PIKE MIRacle ATR sampling accessory with a diamond/ZnSe crystal plate. The spectra were taken in the single reflection mode, over the spectral range 4000–600 cm⁻¹ at 4 cm⁻¹ resolution. Thirty two scans were averaged for the final spectrum, which was afterwards corrected using the ATR correction function within the OPUS 6.0 program. Each ATR

spectrum shown in figures is the average of three ATR spectra acquired per a sample.

Microbial growth assay

Number of viable bacteria on studied paper samples and corresponding soil was determined after 180 days of soil burial experiments. Paper samples were gently rinsed with sterile distilled water, placed into 9 mL of sterile saline, macerated and vortexed prior to decimal dilution in sterile saline. Number of both facultatively anaerobic and obligately anaerobic bacteria was determined on Nutrient agar (*Biolife*) after incubation at 22 °C/3 days in aerobic and anaerobic (*Anaerocult A, Merck*) atmosphere, respectively. Number of viable bacteria was expressed as log CFU (colony forming units) per 1 g of paper sample or wet soil.

Weight loss measurement

Samples degradation was monitored by measuring the weight of paper samples and prints before and after incubation in the soil containers. The samples were taken out and rinsed with distilled water to remove soil particles from the surface. Then they were dried to constant weight and weighed. The weight loss percentage (w) was calculated according to Eq. (1):

$$w = \frac{m_0 - m_1}{m_0} \times 100 / (\%) \quad (1)$$

where m_0 is the initial weight of the sample, m_1 is the final weight of the sample after degradation.

Colour measurement

Colorimetric properties of printed samples before and after biodegradation were measured using the Ocean Optics USB2000+ spectrophotometer and Ocean Optics SpectraSuite software for the calculation of the *CIELAB* values L^* , a^* , b^* from measured reflectance in the entire spectral range (380–730 nm in 1 nm steps). The D50 illuminant and 2° standard observer were applied in these calculations. All the samples were thermostated by the Full Cover water block (EK Water Blocks, EKWB, Slovenia). The temperature of the copper plate surface was varied by circulation of thermostatically controlled water in channels inside the water block, which was assured to be up to 1 °C accurate in the applied temperature

region. All the samples were heated (cooled) and measured at seven different temperatures: 15, 20, 25, 31, 35, 40 and 42 °C.

Results and discussion

Determination of air permeance of tested samples and increase in thickness due to UV print

Table 1 shows the air permeance of the paper samples and increase in thickness of the samples due to UV print. Results show that synthetic paper is not absorbent (air permeance is 0 $\mu\text{m}/\text{Pas}$), unlike recycled and bulky paper. Bulky paper shows the highest values of air permeance (almost 2 times higher compared to recycled paper). Application of UV printing ink onto the surface of recycled and bulky paper completely reduces their air permeance. The increase in thickness of printed bulky paper is the smallest while for synthetic paper is the highest. The measured values of thickness increase due to UV print presented in Table 1 may suggest that different ink amount was applied on papers, but since printing was carried out under the same conditions, these values are result of different ink absorption into the paper structure resulting from physico-chemical composition of paper substrates.

FTIR spectroscopy of thermochromic ink and papers

Figure 1 shows the FTIR spectra of the UV thermochromic ink measured in transmission mode at 25

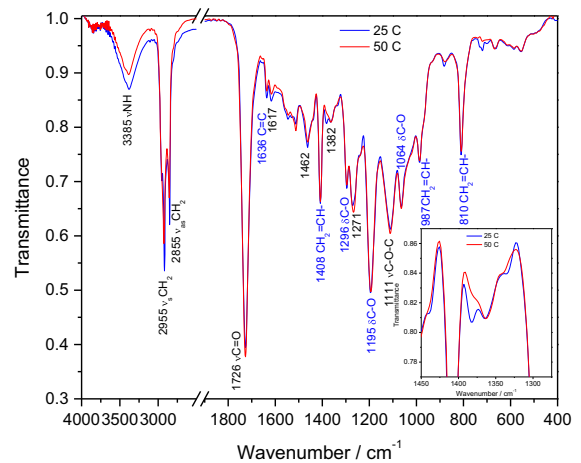


Fig. 1 FTIR spectra of the UV thermochromic ink at 25 and 50 °C, measured in transmission mode

and 50 °C, that is below and above its activation temperature. Even though temperature dependent measurements were accompanied by the thermally induced change in the sample colour, significant changes in the IR spectrum of the UV curable thermochromic ink upon heating were not observed. An exception was a weak band at 1382 cm^{-1} , obtained in the spectrum at the lower temperature and assigned to CH bending vibrations of CH_2 and CH_3 groups, which was missing from the spectrum acquired at the higher temperature due to physical changes such as melting occurring during heating (Fig. 1 inset). Few studies showed that IR spectral changes obtained during heating of the thermochromic composites indicated changes in the molecular structure of the components responsible for the colour change (Hajzeri

Table 1 Air permeance of the samples, increase in thickness of the samples due to UV print and mass ratio of ink to paper

Sample	Air permeance/ ($\mu\text{m}/\text{Pas}$)	Thickness of the paper/ (μm)	Increase in thickness due to UV print/(μm)	Mass ratio ink to paper/(%)
Synthetic paper	0.0 \pm 0.0	96 \pm 1	–	
Synthetic paper-UV print	0.0 \pm 0.0	–	13 \pm 1	25.2
Recycled paper	6.99 \pm 0.25	108 \pm 1	–	
Recycled paper-UV print	0.0 \pm 0.0	–	7 \pm 1	25.1
Bulky paper	13.66 \pm 0.90	125 \pm 1	–	
Bulky paper-UV print	0.0 \pm 0.0	–	5 \pm 1	25.3

et al. 2015; Raditoiu et al. 2016; Panák et al. 2017). The changes occurring during heating of the thermochromic system composed of a leuco dye, corresponding to the symmetric and asymmetric stretching vibrations of COO^- groups which disappear by heating, while the C=O band, characteristic of the colourless lactone form, appears. However, in our case, these changes were not present. Given the similarity between the spectra obtained at both temperatures (Fig. 1), the observed vibrational bands most likely originated from the thermochromic ink resin, and were not the result of the vibrational modes of the thermochromic composites within the microcapsules present in a significantly smaller amount. In addition, due to coverage of microcapsules with polymer resin, the vibrational bands of microcapsules wall material are probably covered and overlapped with vibrational bands of polymer resin that is present in higher amount.

All typical vibrational bands of polyurethane, such as the bands at 3385 cm^{-1} (NH stretching), $2955\text{--}2855\text{ cm}^{-1}$ (symmetric and asymmetric CH_2 stretching), 1726 cm^{-1} (C=O stretching), 1365 cm^{-1} (C-N stretching) and 1111 cm^{-1} (C-O-C stretching) were obtained in the IR spectra, evidencing the existence of polyurethane in the UV thermochromic printing ink (Zhang et al. 2010). In addition to that, the bands at 810 , 987 and 1408 cm^{-1} , attributed to the in-plane and out-of-plane deformation of the vinyl group ($\text{CH}_2=\text{CH-}$), as well as the band at 1636 cm^{-1} , associated with the double bond (C=C) stretching, pointed to the acrylate (Kim and Seo 2004). Moreover, vibrational bands at 1064 , 1195 and 1296 cm^{-1} could be assigned to vibrational modes of functionalities consisting of oxygen atom (C-O stretching), pointing to acrylates as well (Bénard et al. 2008). However, due to complexity of the obtained IR spectra some bands could not be unambiguously assigned. For instance, the sharp bands at 1617 and 1462 cm^{-1} could be associated with the ring stretching modes, implying presence of the phenyl moiety in the structure, most likely of polyurethane (Chalmers 2007). Furthermore, the band at 1462 cm^{-1} could be also assigned to bending of the methylene groups present in both, polyurethane and acrylate, while the band at 1271 cm^{-1} could arise from the C-N stretching and C-O stretching in polyurethane and acrylate, respectively (Chalmers 2007). Nevertheless, the IR spectra

implied that the studied thermochromic printing ink was very likely composed of polyurethane acrylate.

Figure 2 shows the IR spectrum of the unprinted papers. In the IR spectrum of the synthetic paper the obtained bands were associated with polypropylene ($2960\text{--}2840\text{ cm}^{-1}$ (asymmetric and symmetric CH_2 and CH_3 stretching), 1433 cm^{-1} (CH_2 and CH_3 bending)) and calcium carbonate (875 and 712 cm^{-1} (asymmetric and symmetric CO_3^{2-} bending)), while beside calcium carbonate (873 , 709 cm^{-1}) distinctive bands of cellulose (1426 cm^{-1} (in-plane HCH and OCH deformation), $1160\text{--}1000\text{ cm}^{-1}$ (C-O and C-C stretching, COH bending), 898 cm^{-1} (COC and CCO bending)) contributed to the IR spectrum of the recycled paper (Fig. 2) (Proniewicz et al. 2002). The broad band around 3335 cm^{-1} in the spectrum of the recycled paper were assigned to the OH stretching, mostly originating from cellulose hydroxyl groups, though a weak broad band at 1650 cm^{-1} confirmed the presence of water too. In the IR spectrum of bulky paper beside cellulose and calcium carbonate (873 , 710 cm^{-1}), characteristic bands of lignin corresponding to phenyl ring vibrational modes at 1594 cm^{-1} (phenyl stretching), 1272 cm^{-1} (in-plane CH bending) and 812 cm^{-1} (out-of-plane CH bending) were observed (Derkacheva and Sukhov 2008). Comparing the unprinted recycled and bulky paper, the higher intensity of the band assigned to the COC bending of $\beta\text{-(1} \rightarrow 4\text{)-glycosidic}$ linkages, sensitive to the amount of the crystalline versus amorphous structure

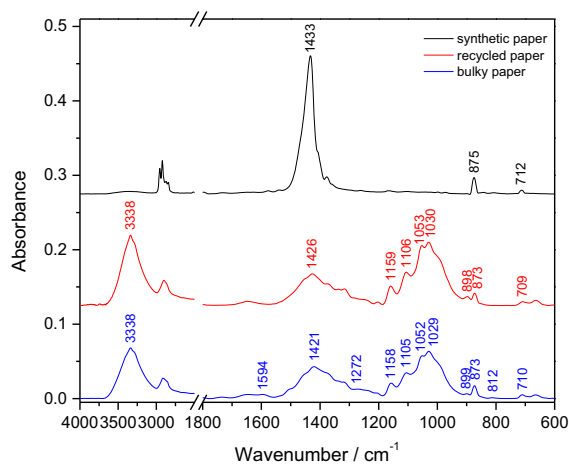


Fig. 2 FTIR spectra of the unprinted papers measured in ATR mode. The spectra of the papers are vertically displaced for visual clarity

of cellulose and also called “amorphous” absorption band, indicated a higher degree of amorphous structure in the recycled paper (898 cm^{-1}) than in the bulky paper (899 cm^{-1}) (Ciolacu et al. 2011).

Optical microscopy

Thermochromic ink is composed of blue microcapsules dispersed in pink conventional screen printing ink and due to that property, when the ink is exposed to temperatures above their activation temperature, the print changes its colour from purple to pink (Fig. 3).

SEM analysis

SEM micrographs of UV print on synthetic paper (Fig. 4) show that microcapsules are covered with polymer resin (binder). After 180 days of biodegradation, the changes in the surface of UV print are observed (Fig. 5). A noticeable biodegradation of the polymer resin can be seen, and the microcapsules become more visible. Figure 5 shows heterogeneous degradation of the print. Microcapsules are in irregular shape, some are notched and some are hollow. In the case of UV prints on recycled and bulky paper (Figs. 6, 7), it can be seen that microcapsules are covered with thinner layer of resin and thus, they are more visible. The number of microcapsules in UV prints is significant and they are in the regular circle forms, with around $1\text{--}2\text{ }\mu\text{m}$ in diameter. After biodegradation, the surfaces are visibly degraded, in

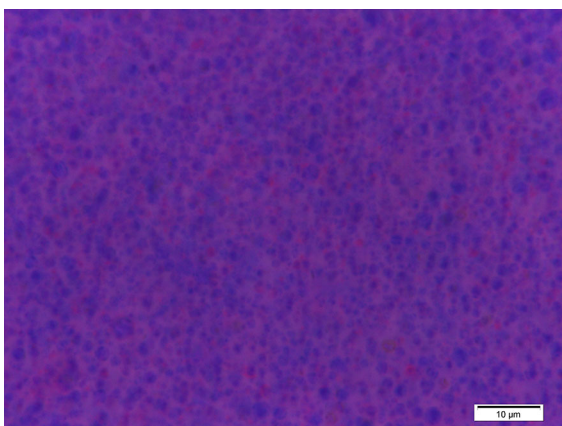


Fig. 3 Optical microscopy image of thermochromic ink at $23\text{ }^{\circ}\text{C}$

UV print on bulky paper more than on UV print on recycled paper. UV print on recycled paper (Fig. 8) shows a larger number of hollow microcapsules than UV print on synthetic paper (Fig. 5), more deformation and higher number of irregular microcapsules. However, the number of microcapsules does not change much more than in the original printed recycled paper (Fig. 6). After 180 days of biodegradation of UV print on bulky paper destruction of almost all microcapsules is visible (Fig. 9). In addition, in Fig. 9 there are also visible cellulose fibres, which indicates a thinning of the polymer resin layer on the surface of bulky paper, i.e. greater biodegradation. From Fig. 9 it can be seen that few microcapsules between cellulose fibres, remains protected. Comparing the results to our previous research where the biodegradation of thermochromic offset prints were studied (Vukoje et al. 2017), results indicated that polymerized ink vehicle (vegetable oil + resin) in thermochromic offset ink is more stable than the polymer resin present in UV curable screen printing thermochromic ink. SEM micrographs indicated a notably higher stability of offset ink binder and accordingly lower deformation of the microcapsules.

Visual evaluation

Figures 10 and 11 show the visual evaluation of printed and unprinted sides of papers before and after biodegradation. After 50 days of biodegradation, the UV prints on all papers show only slight changes in colour (Fig. 10). After 180 days of biodegradation, it can be noticed that surface of UV print on synthetic paper is purple with pink areas, indicating a heterogeneous degradation. The UV print on recycled paper is mostly pink with a very small amount of purple coloration. Only a pink colour is visible for UV print on bulky paper. In the case of UV print on bulky paper it can be noticed that samples after 50 and 180 days were disintegrated into pieces, i.e. showing not only changes in colour, but in the structure as well. The changes in colour of the prints occurring during biodegradations are result of the microcapsules deformation and degradation. The greater the transition to pink colour is, the greater the destruction (deformation) of the microcapsule which was confirmed by SEM micrographs.

Figure 11 shows that unprinted sides of papers before degradation have some differences in colour,

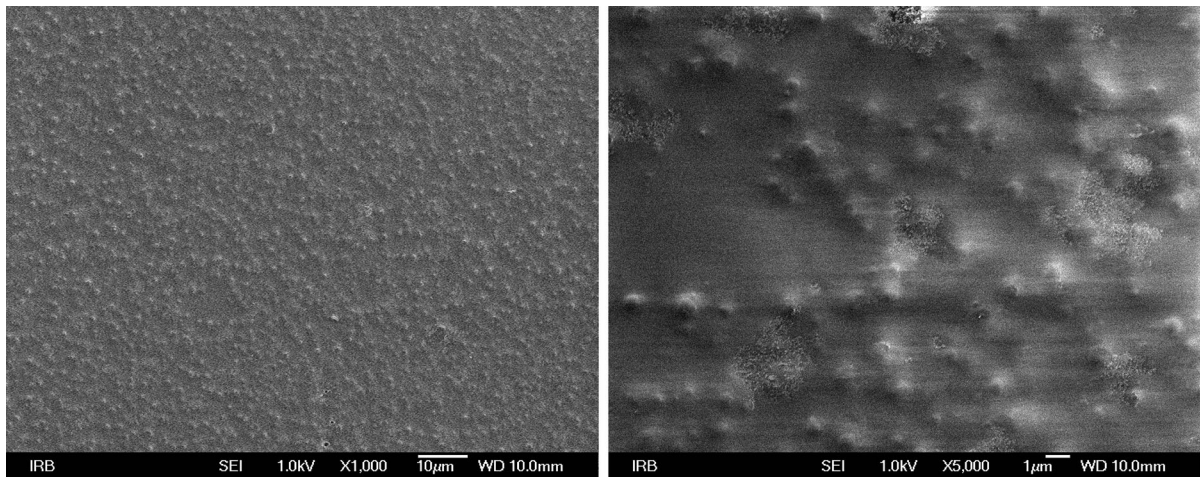


Fig. 4 SEM micrograph of UV print on synthetic paper before biodegradation under different magnifications ($\times 1000$ and $\times 5000$)

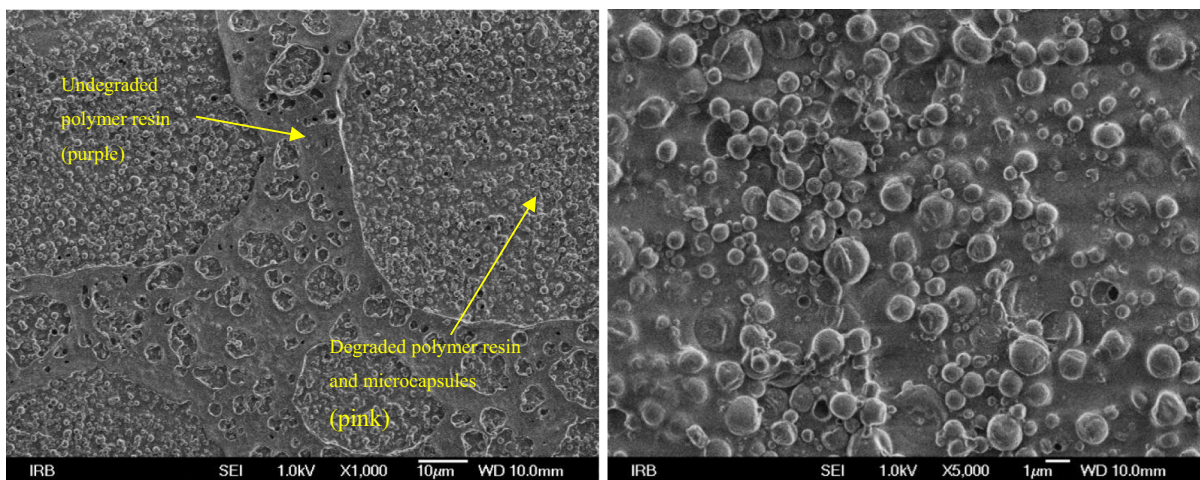


Fig. 5 SEM micrograph of UV print on synthetic paper after 180 days of biodegradation under different magnifications ($\times 1000$ and $\times 5000$)

i.e. unprinted side of recycled paper is pink while unprinted side of bulky paper is more purple. That might be an indication that microcapsules altogether with polymer ink resin penetrate deeper in the structure of bulky paper, promoting biodegradation. In the case of recycled paper, ink binder (altogether with classic pigment) penetrates into its structure. For the print on synthetic paper, there is no penetration of ink into its structure. All components of ink remain on the surface of synthetic paper.

Comparing the unprinted sides of the prints (Fig. 11), UV print on synthetic paper shows almost no changes in its visual appearance. For the UV print

on recycled paper, some formation of spots can be noticed, but after 180 days of biodegradation, these spots present degradation of paper. However, these changes are smaller compared to unprinted side of UV print on bulky paper, whose visual appearance is very diverse from the original.

Microbial growth assay and weight loss measurement

Figure 12 shows the number of bacteria on the unprinted and printed-paper samples after 180 days

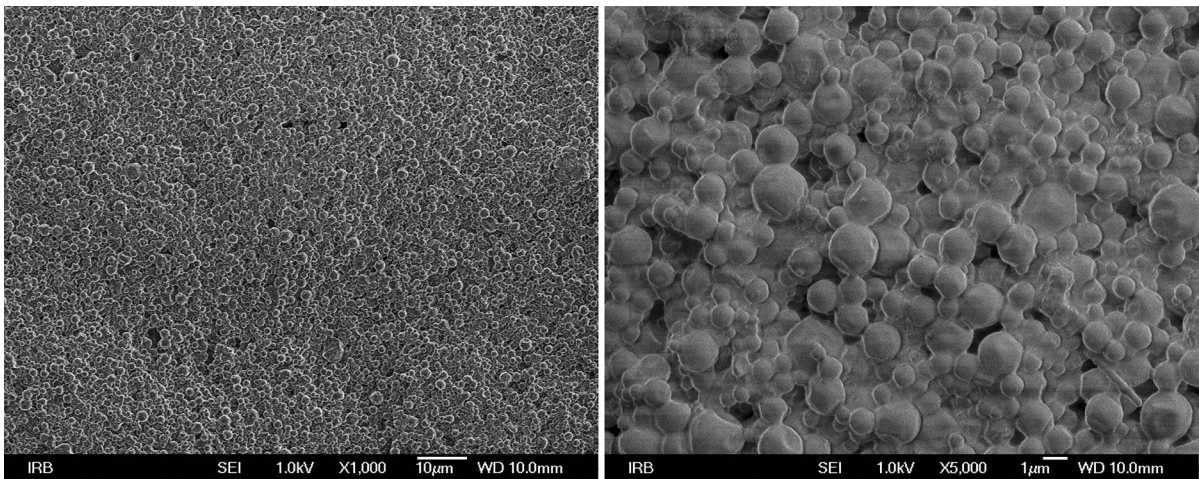


Fig. 6 SEM micrograph of UV print on 33% recycled paper before biodegradation under different magnifications ($\times 1000$ and $\times 5000$)

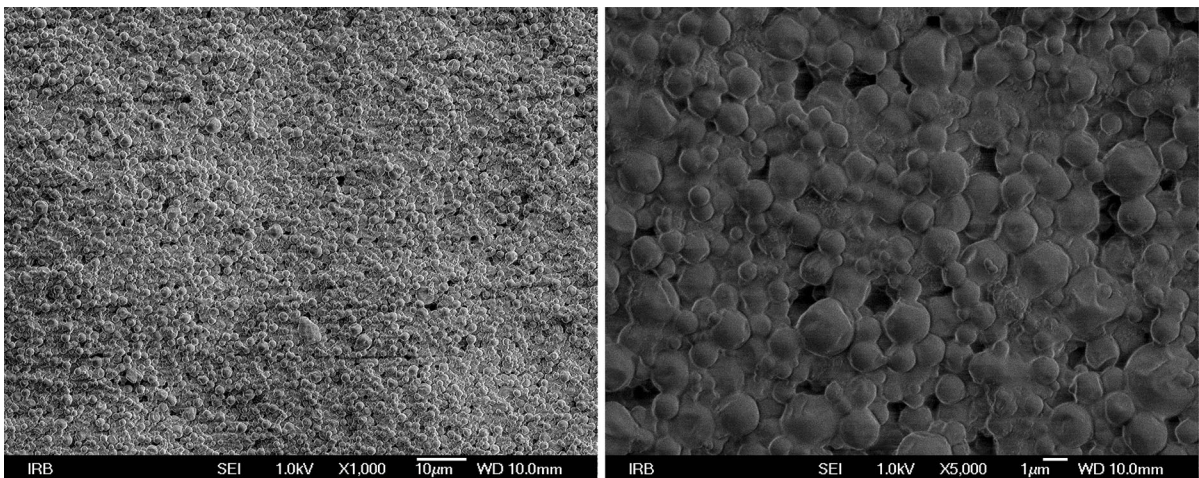


Fig. 7 SEM micrograph of UV print on bulky paper before biodegradation under different magnifications ($\times 1000$ and $\times 5000$)

of biodegradation in the soil. In the case of unprinted paper samples, the highest number of bacteria was obtained on recycled paper, followed by the bulky paper. The number of bacteria obtained on synthetic paper was the smallest and it was smaller compared to number of bacteria isolated from the soil. For this reason, synthetic paper shows no changes in weight after biodegradation period (Table 2), due to microbial attack resistance of polypropylene present in its structure (Arutchelvi et al. 2008; Leja and Lewandowicz 2010). The weight loss measurement for unprinted recycled paper indicates higher biodegradation compared to bulky paper (Table 2). After 180 days of biodegradation, unprinted recycled paper was more

than 90% degraded, while bulky paper was 25.8% degraded. Higher rate of recycled paper biodegradation compared to bulky paper, can be explained by the higher ratio of amorphous cellulose in recycled paper, which was confirmed by FTIR (Fig. 2) and presence of shorter cellulose fibres resulting from process of recycling. Amorphous cellulose is more susceptible to degradation than the crystalline (Van Wyk and Mohulatsi 2003). In addition, bulky paper contains lignin that interferes the paper biodegradation (Komiilis and Ham 2003).

The smallest number of bacteria was isolated on printed synthetic paper and it was almost the same as number of bacteria isolated from the soil, which

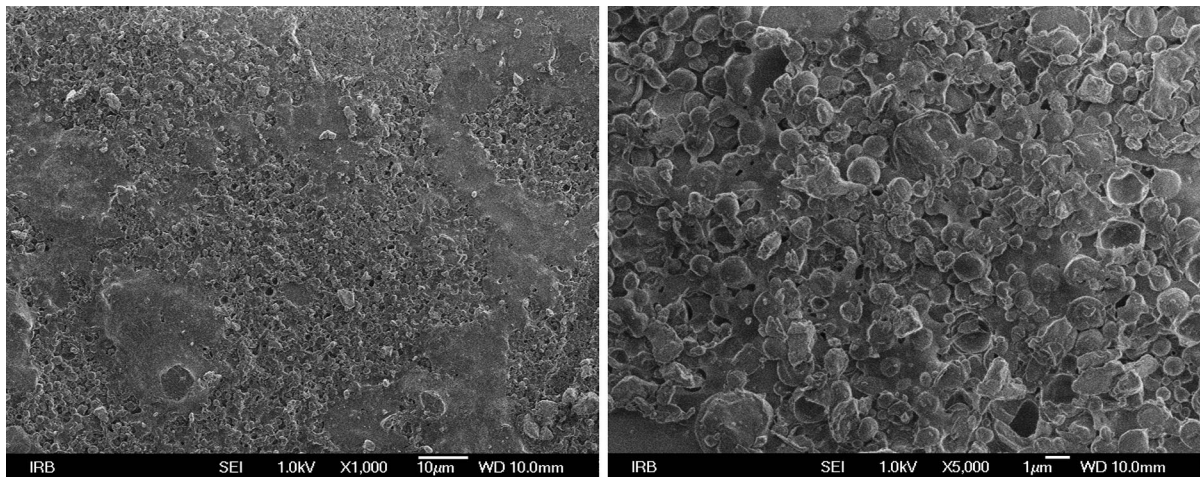


Fig. 8 SEM micrograph of UV print on 33% recycled paper after 180 days of biodegradation under different magnifications ($\times 1000$ and $\times 5000$)

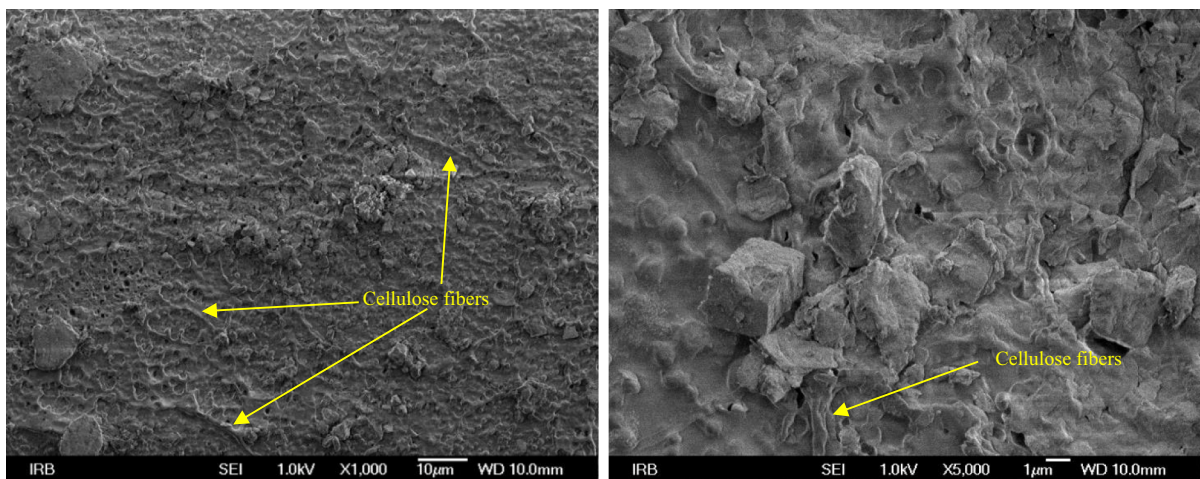


Fig. 9 SEM micrograph of UV print on bulky paper after 180 days of biodegradation under different magnifications ($\times 1000$ and $\times 5000$)

resulted in a small weight loss (3%) after 180 days of biodegradation (Table 2). This can be mainly described by the UV print degradation rather than synthetic paper degradation since unprinted synthetic paper shows no changes in weight during biodegradation. It can be assumed that UV print is more biodegradable than synthetic paper. For the printed recycled paper an opposite behaviour was observed, i.e. notable reduction of biodegradation rate compared to unprinted recycled paper was noticed. With the application of thermochromic ink, the weight loss was five times lower. This behaviour can be explained by the polymer ink resin and pigment absorption. In the

case of recycled paper, it is obvious that classic pigment that penetrates into its structure lowers the rate of biodegradation, which means that classic pigment is less degradable than recycled paper.

The highest change in the weight loss was obtained for the printed bulky paper. In this case, printed bulky paper degrades faster than unprinted bulky paper. Higher rate of printed bulky paper biodegradation compared to printed recycled paper can be due to better absorption of microcapsules. The deeper the penetration of the microcapsule into to structure of paper is, higher biodegradation occurring from the unprinted side is. Considering the fact that the weight

Fig. 10 Visual evaluation of prints before and after 50 and 180 days of biodegradation



Fig. 11 Visual evaluation of prints before and after 50 and 180 days of biodegradation—unprinted side



loss measurement for printed sample is almost the same after 50 and 180 days of biodegradation, degradation of paper probably stopped after 50 days, but after that period only degradation of microcapsules

occurred. Due to their small sizes and lower share in the thermochromic ink and printed sample, the weight loss increase after 180 days was negligible. The similar number of bacteria obtained for unprinted

Fig. 12 Number of viable bacteria on unprinted and printed-paper samples and in corresponding soil after 180 days of biodegradation

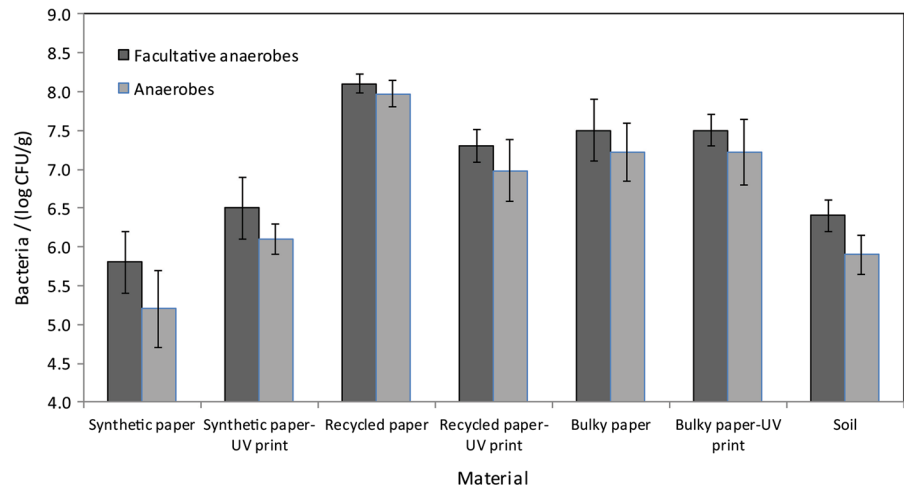


Table 2 Weight loss during soil burial

Sample	Weight loss/(%)	
	Days	
	50	180
Synthetic paper	0.0	0.0
Synthetic paper-UV print	0.6	3.0
Recycled paper	46.3	92.9
Recycled paper-UV print	6.8	17.8
Bulky paper	20.5	25.8
Bulky paper-UV print	49.2	50.2

and printed bulky paper can be explained by the fact that bacterial growth after 180 days of biodegradation of printed bulky paper was probably in decline due to destruction of almost all microcapsules (Fig. 9) and reduction in biodegradation rate.

Thermochromic microcapsules are mostly composed of urea-formaldehyde or melamine-formaldehyde resins gelatine-gum arabic and epoxy resins (Aitken et al. 1996; Fujinami 1996; Seebth and Lotzsch 2008) which are biodegradable and during biodegradation can act as nitrogen sources (El-Sayed et al. 2006). Microcapsules can act as an active sites promoting biodegradation.

FTIR spectroscopy of prints before and after biodegradation

The IR spectra of the thermochromic prints on all paper samples: synthetic, bulky and recycled, measured in attenuated total reflectance (ATR) mode, were very similar (Fig. 13). In comparison to the spectrum of the thermochromic UV curable ink, the bands at 1408, 1296, 1271, 1195 and 1064 cm^{-1} in the IR spectra of the prints were weaker and poorly defined. The intensity of these bands decreased due to polymerization of polyurethane acrylate during UV curing.

The IR spectra of the thermochromic UV prints on the used papers before and after 50 and 180 days of biodegradation are shown in Figs. 14, 15 and 16. In

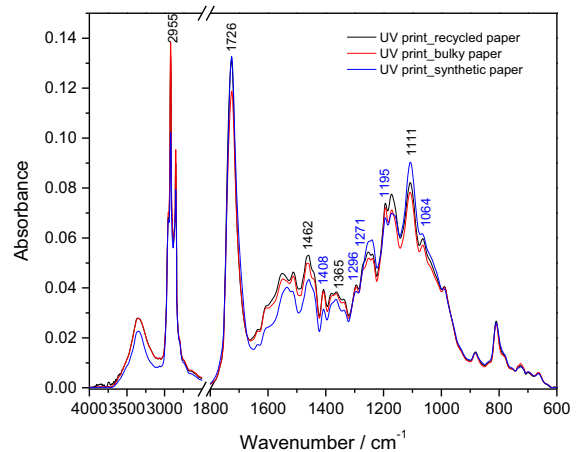


Fig. 13 FTIR spectra of the UV thermochromic print on the recycled, bulky and synthetic paper before biodegradation, measured in ATR mode

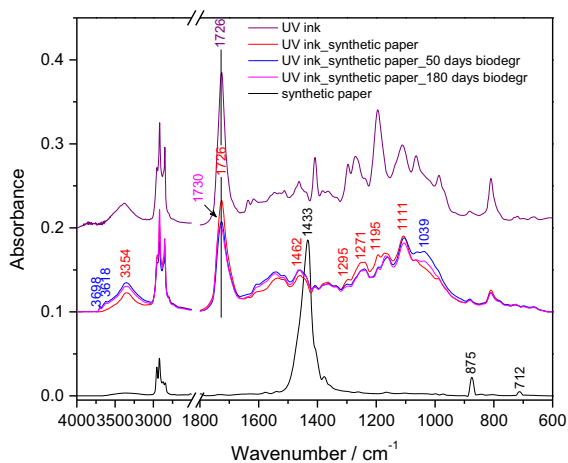


Fig. 14 FTIR spectra of the UV thermochromic ink, the neat synthetic paper and the prints of the ink on the synthetic paper before and after 50 and 180 days of biodegradation, measured in ATR mode. The spectra of the ink, the paper and the prints are vertically displaced for visual clarity

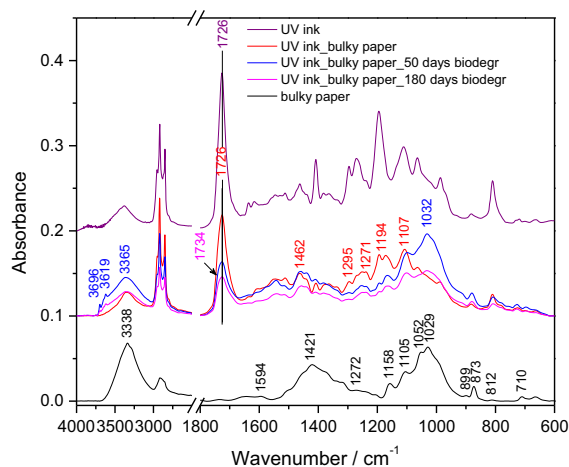


Fig. 16 FTIR spectra of the thermochromic ink, the neat bulky paper and the prints of the ink on the bulky paper before and after 50 and 180 days of biodegradation, measured in ATR mode. The spectra of the ink, the paper and the prints are vertically displaced for visual clarity

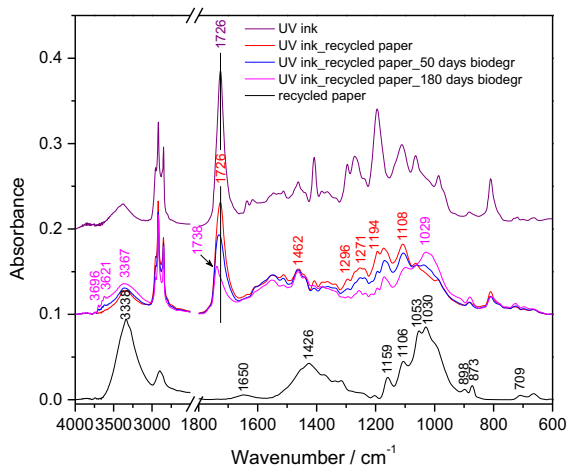


Fig. 15 FTIR spectra of the thermochromic ink, the neat recycled paper and the prints of the ink on the recycled paper before and after 50 and 180 days of biodegradation, measured in ATR mode. The spectra of the ink, the paper and the prints are vertically displaced for visual clarity

addition, the IR spectra of UV curable ink and unprinted papers have been presented in Figs. 12, 13 and 14.

A decrease of band intensities located in the 1100–1000 cm⁻¹ range (attributed to the ester C–O stretching vibration), 1260–1200 cm⁻¹ range (attributed to carbonyl oxygen linkage) and carbonyl peak around 1730 cm⁻¹ were observed after degradation. The changes in those bands are present for all

printed papers after biodegradation (Figs. 14, 15 and 16) and very likely indicate the breaking down of the ester linkages, leading to the changes in the ester and urethane groups of polyurethane resin, i.e. changes in polymeric structure (Oprea and Doroftei 2011; Oprea et al. 2016). In the ranges of 1100–1000 cm⁻¹ and 1260–1200 cm⁻¹, the highest changes were observed for the print on bulky paper, followed by print on recycled paper. The smallest changes were observed for the synthetic paper. However, the changes in the spectral range of 1300–1800 cm⁻¹ were observed only for the printed bulky paper.

An appearance of the intense broad band at around 1030 cm⁻¹ could be attributed to cellulose, due to thinning of the polymer resin on the surface of the bulky and recycled paper, which can be attributed to stretching of C–O in cellulose/hemicellulose molecules (Grilj et al. 2012). Interestingly, in the IR spectrum of the UV print on the bulky paper this band decreased after 180 days of biodegradation, if compared to the spectrum after 50 days, indicating cellulose degradation as well. This was supported by SEM micrographs (Figs. 7 and 9). The intense cellulose like vibration bands (at 1030 cm⁻¹) were also obtained after 180 days of the UV print biodegradation on the recycled paper. Given that the spectral motif around 1030 cm⁻¹ was obtained in the IR spectra of the UV print on all the papers after biodegradation, including the synthetic paper not consisting of cellulose, its

origin could be also partially associated with silicates (Si–O stretching) adsorbed on the prints from the soil. The presence of silicates on the surface of the prints, was also indicated by the weak bands at 3698 and 3618 cm^{-1} assigned to O–H stretching in the Si–OH structural moieties located on the silicate surface (Das et al. 2013; Tinti et al. 2015). Since weak bands around 3696 and 3620 cm^{-1} corresponding to the silicates OH groups were obtained in the IR spectra of the prints on all the papers, it was very likely that the band at 1039 cm^{-1} associated with the Si–O stretching in silicates was also present in the spectra of the prints on the recycled and bulky paper, but overlapped by the strong broad cellulose band.

Due to degradation of polyurethane, the formation of degradation products can be noticed and followed in the hydroxyl and NH group stretching range (3600–3100 cm^{-1}), whose intensity increased after biodegradation (Bénard et al. 2008; Oprea and Doroftei 2011; Huang et al. 2016). Compared to the IR spectra before biodegradation, the band at around 3350 cm^{-1} was slightly stronger, wider and positioned at higher wavenumbers in the spectra of the buried prints (Figs. 14, 15 and 16).

Colorimetric measurements

Results of colorimetric a^* and b^* values determined on UV thermochromic prints before and after biodegradation are presented in Fig. 17. In the *CIELAB* colour space the value L^* represents the lightness of the colour, the value $+a^*$ represents redness, $-a^*$ represents greenness, $+b^*$ represents yellowness while the value $-b^*$ represents blueness. Due to the formation of polymer ink layer on the surface of all papers and its complete coverage of paper samples, the colour of unprinted papers does not have a significant influence on the colour reproduction of the UV prints. Figure 17 shows that the colorimetric a^* and b^* values of original UV prints on bulky and recycled paper, measured below the activation temperature, have similar colorimetric properties. Compared to UV prints on bulky and recycled paper, UV print on synthetic paper has higher a^* value, and smaller b^* value, due to higher concentration of ink on the surface of the paper. Figure 17 shows the transition of prints colour from purple to pink. The a^* and b^* values of UV prints after 50 days of biodegradation

are smaller than the initial values. The a^* value on bulky paper print shows the lowest positive values while the b^* value shows the smallest negative values, indicating the highest colour change. After 180 days of biodegradation, the a^* and b^* values of all samples, are more positive compared to the initial values. The smallest colour change was in the case of UV print on synthetic paper. After 180 days of biodegradation, the pink colour of print on bulky paper was lighter (smaller a^* value) compared to print on recycled paper, indicating higher colour change.

The TC system has memory, which is called hysteresis. It's colour hysteresis describes the colour of a TC sample as a function of temperature and should be presented in four-dimensional space (i.e. whose three dimensions represent colour values L^* , a^* , b^* , while the fourth dimension illustrates temperature (T)) or by two-dimensional graphs (Kulčar et al. 2010). The trajectory obtained by heating is not equal to one obtained by cooling. The area of the surface defined by the two trajectories shows the similarity (of the colour change) of the heating and cooling run.

The reversible TC process can be presented by change of L^* , a^* and b^* values as a function of temperature. When printed sample is heated, decolourization of microcapsules occurs above the activation temperature (TA). Therefore, the b^* values increase because only the pink colour of the classic pigment remains. The reverse process occurs during cooling at lower temperatures.

$L^*(T)$ hysteresis describes temperature dependence of L^* values. Figure 18a shows that all UV prints before biodegradation tests show similar values, i.e. similar reversibility of colour. UV prints on recycled and bulky paper show almost the same behaviour, while small differences can be noticed for UV print on synthetic paper. Due to higher amount of polymer resin containing pink classic pigment over the microcapsules present on the surface of the synthetic paper, the hysteresis is shifted to higher L^* values. After 50 days of biodegradation (Fig. 18b), the initial L^* values of the UV prints on recycled and bulky paper are shifted to higher L^* values, similar to L^* value of UV print on synthetic paper. This indicates a higher concentration of classic pink pigment on their surface. The highest decrease of $L^*(T)$ hysteresis height was obtained on printed bulky paper, while the smallest change in $L^*(T)$ hysteresis height was obtained on printed synthetic paper, indicating that the highest

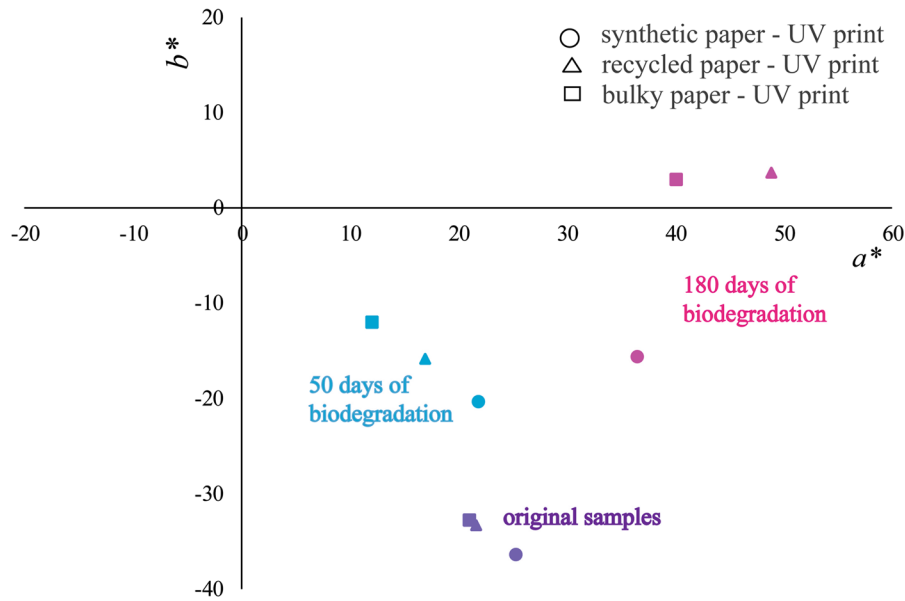


Fig. 17 Colorimetric properties (a^* and b^* values) of UV prints measured at 20 °C before (purple), after 50 days (blue) and 180 days (pink) of biodegradation (circle—UV print on

synthetic paper, triangle—UV print on recycled paper, square—UV print on bulky paper). (Color figure online)

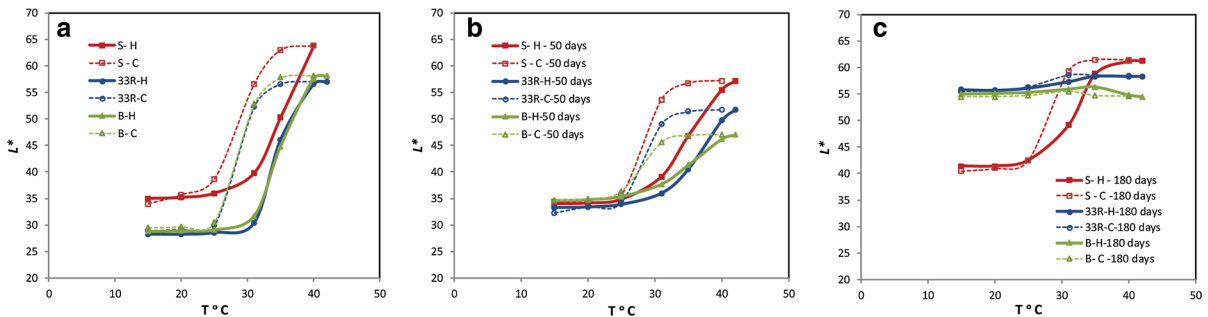


Fig. 18 CIELAB L^* values of UV print on synthetic paper (S—red), recycled paper (33R—blue) and bulky paper (B—green) in dependence on temperature at heating (solid line) and cooling

(open line) before biodegradation (a), after 50 days of biodegradation (b) and after 180 days of biodegradation (c). (Color figure online)

destruction of colour (microcapsules) was noticed on printed bulky paper. After 180 days of biodegradation (Fig. 18c), the prints on recycled and bulky papers showed remarkable reduction of thermochromic effect. The reduction of thermochromic effect and changes occurring in $L^*(T)$ hysteresis are result of reduction in active microcapsules number, which was confirmed by the SEM micrographs. $L^*(T)$ hysteresis are substantially shifted toward higher L^* values suggesting greater concentration of classic pink pigment in relation to the concentration of microcapsules.

In addition, the changes occurring in $b^*(T)$ hysteresis may also point to degradation of blue microcapsules (Fig. 19a–c). The smallest changes occurring in

$b^*(T)$ hysteresis were obtained for UV print on synthetic paper. Interestingly, after 50 days of biodegradation, the final b^* values (at highest temperatures) are not approaching to zero by heating, but they are becoming positive (shift to the yellow area). In the case of UV prints on recycled and bulky paper, the b^* values are positive throughout the whole temperature range. After 180 days of biodegradation, the greatest shift to yellow area was obtained on printed synthetic paper, followed by printed recycled paper and printed bulky paper (Fig. 19c).

After 180 days of biodegradation, the final a^* values (at highest temperatures) are the highest in the case of printed synthetic paper, slightly lower values

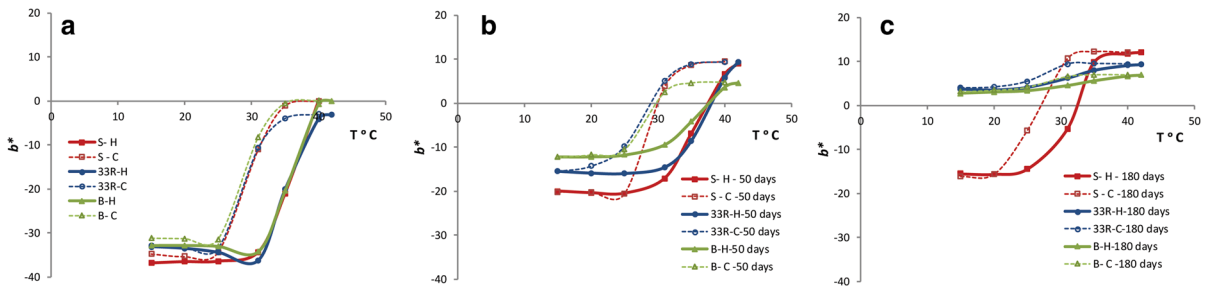


Fig. 19 CIELAB b^* values of UV print on synthetic paper (S—red), recycled paper (33R—blue) and bulky paper (B—green) in dependence on temperature at heating (solid line) and cooling

(open line) before biodegradation (a), after 50 days of biodegradation (b) and after 180 days of biodegradation (c). (Color figure online)

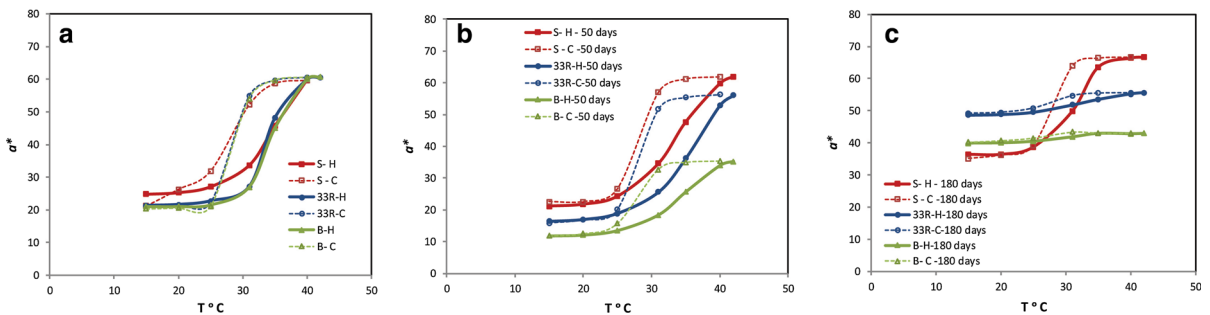


Fig. 20 CIELAB a^* values of UV print on synthetic paper (S—red), recycled paper (33R—blue) and bulky paper (B—green) in dependence on temperature at heating (solid line) and cooling

(open line) before biodegradation (a), after 50 days of biodegradation (b) and after 180 days of biodegradation (c). (Color figure online)

are on printed recycled paper, and the smallest a^* values are on printed bulky paper (Fig. 20a–c). Accordingly, the highest shift to yellow and red area obtained on the printed synthetic paper indicates the highest concentration of classic pink pigment. It can be assumed that classical pink pigment shows slower rate of biodegradation. In the case of printed bulky paper, in which the highest absorption of thermochromic ink was noticed, the active sites (microcapsules) that bacteria use for their metabolism are the most accessible. If the effect of ink separation is smaller, these sites are less accessible, so the rate of biodegradation is lower.

Conclusions

The ink penetration into the paper structure is a very important property. Results show that the best absorption of ink is for the bulky paper structure, followed by recycled paper. The structure of synthetic paper was not penetrated by the ink. The results show that the

print obtained on paper that absorbs more biodegradable thermochromic ink, shows higher rate of biodegradation. The more the microcapsules are exposed to bacteria, i.e. covered with a thinner layer of ink polymer resin, the higher rate of biodegradation will be. On synthetic paper, the microcapsules are covered with a thicker layer of polymer resin making them less exposed to bacteria. The FTIR spectra were interpreted to indicate that the ink binder is polymer resin containing polyurethane acrylate. The highest changes in the IR spectra during biodegradation were obtained for UV print on bulky paper followed by UV print on recycled paper. The smallest changes were obtained for the UV print on synthetic paper. In addition, the SEM micrograph indicated degradation of almost all microcapsules after 180 days of biodegradation on UV print on bulky paper. The SEM micrograph of prints on recycled paper after 180 days of biodegradation showed a certain deformation and degradation of microcapsules. In the case of UV print on synthetic paper, in the SEM micrograph only degradation of polymer resin was observed.

However, deformation of microcapsules can be noticed but not in the whole area as for UV print on recycled paper. Some of the microcapsules remain protected by the polymer resin hence biodegradation occurred as spots, thus the colour degradation of print after 180 days of biodegradation was less comparable to other samples on bulky and recycled paper. Based on the obtained results, it can be said that in the case of the used thermochromic UV ink, the polymer resin, pigment and the microcapsules are ultimately biodegradable in the anaerobic soil environment.

Acknowledgments The authors are grateful for the support of University of Zagreb, Grant No. TP122 and Croatian Science Foundation (Project No. IP-2014-09-5656).

References

- Aitken D, Burkinshaw SM, Griffiths J et al (1996) Textile applications of thermochromic systems. *Rev Prog Color* 26:1–8
- Arutchelvi J, Sudhakar M, Arkatkar A et al (2008) Biodegradation of polyethylene and polypropylene. *Indian J Biotechnol* 7:9–22
- Bardi MAG, Munhoz MML, Auras RA, Machado LDB (2014) Assessment of UV exposure and aerobic biodegradation of poly(butylene adipate-co-terephthalate)/starch blend films coated with radiation-curable print inks containing degradation-promoting additives. *Ind Crops Prod* 60:323–334. <https://doi.org/10.1016/j.indcrop.2014.06.042>
- Bénard F, Mailhot B, Mallet J, Gardette JL (2008) Photocuring of an electron beam cured polyurethane acrylate resin. *Polym Degrad Stab* 93:1122–1130. <https://doi.org/10.1016/j.polymdegradstab.2008.03.008>
- Carré B, Magnin L, Ayala C (2005) Digital prints: a survey of the various deinkability behaviors. In: Proceedings of the 7th research forum on recycling, PAPTAC, Quebec, Canada, pp 1–11
- Chalmers JM (2007) Spectra-structure correlations: polymer spectra. In: Griffiths PM, Chalmers JM (eds) *Handbook of vibrational spectroscopy*. Wiley, Chichester
- Ciolacu D, Ciolacu F, Popa VI (2011) Amorphous cellulose—structure and characterization. *Cellul Chem Technol* 45:13–21. <https://doi.org/10.1163/156856198X00740>
- Das G, Kalita RD, Deka H et al (2013) Biodegradation, cytocompatibility and performance studies of vegetable oil based hyperbranched polyurethane modified biocompatible sulfonated epoxy resin/clay nanocomposites. *Prog Org Coat* 76:1103–1111. <https://doi.org/10.1016/j.porgcoat.2013.03.007>
- De la Cruz FB, Yelle DJ, Gracz HS, Barlaz MA (2014) Chemical changes during anaerobic decomposition of hardwood, softwood, and old newsprint under mesophilic and thermophilic conditions. *J Agric Food Chem* 62:6362–6374. <https://doi.org/10.1021/jf501653h>
- Derkacheva O, Sukhov D (2008) Investigation of lignins by FTIR spectroscopy. *Macromol Symp* 265:61–68. <https://doi.org/10.1002/masy.200850507>
- El-Sayed WS, El-Baz AF, Othman AM (2006) Biodegradation of melamine formaldehyde by *Micrococcus* sp. strain MF-1 isolated from aminoplastic wastewater effluent. *Int Biodeterior Biodegrad* 57:75–81. <https://doi.org/10.1016/j.ibiod.2005.11.006>
- Erhan SZ, Bagby MO (1995) Vegetable-oil-based printing ink formulation and degradation. *Ind Crops Prod* 3:237–246. [https://doi.org/10.1016/0926-6690\(94\)00040-6](https://doi.org/10.1016/0926-6690(94)00040-6)
- Erhan SZ, Bagby MO, Nelsen TC (1997) Statistical evaluation of biodegradation of news ink vehicles and ink formulations. *J Am Oil Chem Soc* 74:707–712
- Fujinami F (1996) Ultraviolet-curable thermochromic ink composition. U.S. Patent 5,500,040, 19 March 1996
- Grilj S, Klanjšek Gunde M, Szentgyörgyvölgyi R, Gregor-Svetec D (2012) FT-IR and UV/VIS analysis of classic and recycled papers. *Papiripar LVI* 4:7–13
- Hajzeri M, Bašneć K, Bele M, Klanjšek Gunde M (2015) Influence of developer on structural, optical and thermal properties of a benzofluoran-based thermochromic composite. *Dye Pigment* 113:754–762. <https://doi.org/10.1016/j.dyepig.2014.10.014>
- Hermann BG, Debeer L, De Wilde B et al (2011) To compost or not to compost: carbon and energy footprints of biodegradable materials' waste treatment. *Polym Degrad Stab* 96:1159–1171. <https://doi.org/10.1016/j.polymdegradstab.2010.12.026>
- Homola TJ (2008) Color-changing inks. AccessScience. McGraw-Hill Education, New York
- Hoshino A, Kanao S, Fukushima K et al (2003) Influence of surface printing materials on the degradability of biodegradable plastic films in soil. *Soil Sci Plant Nutr* 49:903–907. <https://doi.org/10.1080/00380768.2003.10410354>
- Huang J, Sun J, Zhang R et al (2016) Improvement of biodegradability of UV-curable adhesives modified by a novel polyurethane acrylate. *Prog Org Coat* 95:20–25. <https://doi.org/10.1016/j.porgcoat.2016.02.017>
- Kim DS, Seo WH (2004) Ultraviolet-curing behavior and mechanical properties of a polyester acrylate resin. *J Appl Polym Sci* 92:3921–3928. <https://doi.org/10.1002/app.20422>
- Komilis DP, Ham RK (2003) The effect of lignin and sugars to the aerobic decomposition of solid wastes. *Waste Manag* 23:419–423. [https://doi.org/10.1016/S0956-053X\(03\)00062-X](https://doi.org/10.1016/S0956-053X(03)00062-X)
- Kulčar R, Friskovec M, Hauptman N et al (2010) Colorimetric properties of reversible thermochromic printing inks. *Dye Pigment* 86:271–277. <https://doi.org/10.1016/j.dyepig.2010.01.014>
- Leach RH (2007) *The printing ink manual*, 5th edn. Springer, Dordrecht
- Leja K, Lewandowicz G (2010) Polymer biodegradation and biodegradable polymers—a review. *Pol J Environ Stud* 19:255–266
- López Alvarez JV, Larrucea MA, Bermúdez PA, Chicote BL (2009) Biodegradation of paper waste under controlled composting conditions. *Waste Manag* 29:1514–1519. <https://doi.org/10.1016/j.wasman.2008.11.025>

- Monte MC, Fuente E, Blanco A, Negro C (2009) Waste management from pulp and paper production in the European Union. *Waste Manag* 29:293–308. <https://doi.org/10.1016/j.wasman.2008.02.002>
- Oprea S, Doroftei F (2011) Biodegradation of polyurethane acrylate with acrylated epoxidized soybean oil blend elastomers by *Chaetomium globosum*. *Int Biodeterior Biodegrad* 65:533–538. <https://doi.org/10.1016/j.ibiod.2010.09.011>
- Oprea S, Potolinca VO, Gradinariu P et al (2016) Synthesis, properties, and fungal degradation of castor-oil-based polyurethane composites with different cellulose contents. *Cellulose* 23:2515–2526. <https://doi.org/10.1007/s10570-016-0972-4>
- Panák O, Držková M, Kaplanová M et al (2017) The relation between colour and structural changes in thermochromic systems comprising crystal violet lactone, bisphenol A, and tetradecanol. *Dye Pigment* 136:382–389. <https://doi.org/10.1016/j.dyepig.2016.08.050>
- Pivnenko K, Eriksson E, Astrup TF (2015) Waste paper for recycling: overview and identification of potentially critical substances. *Waste Manag* 45:134–142. <https://doi.org/10.1016/j.wasman.2015.02.028>
- Proniewicz LM, Paluszkiwicz C, Weselucha-Birczyńska A et al (2002) FT-IR and FT-Raman study of hydrothermally degraded groundwood containing paper. *J Mol Struct* 614:345–353. [https://doi.org/10.1016/S0022-2860\(02\)00275-2](https://doi.org/10.1016/S0022-2860(02)00275-2)
- Raditoiu A, Raditoiu V, Nicolae CA et al (2016) Optical and structural dynamical behavior of crystal violet lactone-phenolphthalein binary thermochromic systems. *Dye Pigment* 134:69–76. <https://doi.org/10.1016/j.dyepig.2016.06.046>
- Robert T (2015) “green ink in all colors”—printing ink from renewable resources. *Prog Org Coat* 78:287–292. <https://doi.org/10.1016/j.porgcoat.2014.08.007>
- Seeboth A, Lotzsch D (2008) Thermochromic phenomena in polymers. Smithers Rapra Technology Limited, Shropshire
- Seeboth A, Lotzsch D (2013) Thermochromic and thermotropic materials. CRC Press, Boca Raton
- Seeboth A, Klukowska A, Ruhmann R, Löttsch D (2007) Thermochromic polymer materials. *Chin J Polym Sci* 25:123–135. <https://doi.org/10.1142/S0256767907001923>
- Shah AA, Hasan F, Hameed A, Ahmed S (2008) Biological degradation of plastics: a comprehensive review. *Biotechnol Adv* 26:246–265. <https://doi.org/10.1016/j.biotechadv.2007.12.005>
- Shogren RL, Petrovic Z, Liu Z, Erhan SZ (2004) Biodegradation behavior of some vegetable oil-based polymers. *J Polym Environ* 12:173–178. <https://doi.org/10.1023/B:JOOE.0000038549.73769.7d>
- Stinson JA, Ham RK (1995) Effect of lignin on the anaerobic decomposition of cellulose as determined through the use of a biochemical methane potential method. *Environ Sci Technol* 29:2305–2310. <https://doi.org/10.1021/es00009a023>
- Tang SLP, Stylios GK (2006) An overview of smart technologies for clothing design and engineering. *Int J Cloth Sci Technol* 18:108–128. <https://doi.org/10.1108/09556220610645766>
- Thompson B (2004) Printing materials: science and technology, 2nd edn. Pira International Press, Leatherhead
- Tinti A, Tugnoli V, Bonora S, Francioso O (2015) Recent applications of vibrational mid-infrared (IR) spectroscopy for studying soil components: a review. *J Cent Eur Agric* 16:1–22. <https://doi.org/10.5513/JCEA01/16.1.1535>
- Van Wyk JPH, Mohulatsi M (2003) Biodegradation of waste cellulose. *J Polym Environ* 11:23–28. <https://doi.org/10.1023/A:1023883428359>
- Venelampi O, Weber A, Rönkkö T, Itävaara M (2003) The biodegradation and disintegration of paper products in the composting environment. *Compost Sci Util* 11:200–209. <https://doi.org/10.1080/1065657X.2003.10702128>
- Vukoje M, Rožić M, Miljanić S, Pasanec Preprotić S (2017) Biodegradation of thermochromic offset prints. *Nord Pulp Pap Res J* 32:289–298. <https://doi.org/10.3183/NPPRJ-2017-32-02-p289-298>
- Wang X, De la Cruz FB, Ximenes F, Barlaz MA (2015) Decomposition and carbon storage of selected paper products in laboratory-scale landfills. *Sci Total Environ* 532:70–79. <https://doi.org/10.1016/j.scitotenv.2015.05.132>
- Zhang T, Wu W, Wang X, Mu Y (2010) Effect of average functionality on properties of UV-curable waterborne polyurethane-acrylate. *Prog Org Coat* 68:201–207. <https://doi.org/10.1016/j.porgcoat.2010.02.004>